Cite this: DOI: 10.1039/c0xx00000x

www.rsc.org/xxxxxx

ARTICLE TYPE

Equiatomic Ternary Chalcogenide: PdPS and Its Reduced Graphene Oxide Composite for Efficient Electrocatalytic Hydrogen Evolution

Sujoy Sarkar and Srinivasan Sampath*

Received (in XXX, XXX) Xth XXXXXXXXX 20XX, Accepted Xth XXXXXXXXX 20XX
DOI: 10.1039/b000000x

The layered ternary chalcogenide, palldium phosphorous sulphide (PdPS) and its composite with reduced graphene oxide are shown to be efficient hydrogen evolution electrocatalysts. The Tafel slope and the exchange current density values associated with hydrogen evolution reaction are determined to be 46 mVdec^{-1} and 1.4x10^{-4}Acm^{-2} respectively.

Hydrogen as a promising fuel has generated enormous interest in its production through various routes.[1]The electrochemical route of generation of hydrogen from water using platinum and non-Pt catalysts has received considerable attention[2] and the evolution of H_2 can be modulated using the applied voltage. The so-called 'Volcano plot'[3-4] that relates the free energy of hydrogen adsorption on various materials with the exchange current density leads to platinum being the best electrocatalyst based on its thermoneutrality. There are various electrode materials based on chalcogenides,[5] particularly molybdenum and tungsten sulphides,[6] selenides,[7] phosphides,[8] carbides,[9] borides,[10] and (bi)metallic[11] systems that have been proposed as efficient hydrogen evolution catalysts. Molybdenum sulphide has received maximum attention in recent years. It is reported to be inactive in the bulk form towards electrochemical hydrogen evolution[12] but is found to be very active when the size is reduced to nanoscale.[13] The reason attributed to the bulk form being inactive is the possible intercalation of hydrogen.[12] The proposed active sites in MoS_2 are the "sulphur' edges that effectively adsorb H atoms and mediates hydrogen evolution, leading to excellent HER activity.[14] The composites of chalcogenides with graphene or reduced graphene oxide (rGO) are shown to be very good catalysts[15-16] as compared to their individual counterparts though the interactions between the constituents are not clear at present. The use of nickel phosphide has recently been reported.[8] Metallic Pd is known to be a very good hydrogen evolution catalyst[4] based on its enthalpy of hydrogen adsorption being close to that of Pt and the consequent electroneutrality for free energy of hydrogen adsorption. Pasti et al.[17] have correlated the position of the d-band centers of the catalyst with respect to the Fermi level to its affinity towards species such as H, CO and O. Based on DFT calculations, it is concluded that Pd or Pd overlayers on other noble metals lead to high energy for hydrogen adsorption. Bulk Pd which is active for hydrogen splitting is also conducive for hydrogen solubility under appropriate conditions of pressure and temperature[18] that lead to lattice expansion and formation of hydride phases causing instability. Alloying of Pd or palladium-based compounds may suppress the formation of hydride.[19]

In the present studies, we report a novel phosphochalcogenide containing S, P and Pd, as a catalyst for HER. Bither et al.[20] and subsequently Jeitschko[21] have synthesized and studied the crystal chemistry of PdPS. The electrical and optical properties reveal that PdPS is an indirect band gap semiconductor with a band gap of 1.45 eV. The crystal structure of PdPS reveals that there is no clear van der Waal's gap present unlike MoS_2. The PdPS structure involves mixed stacking sequence alternating between PdP_2 and PdS_2. The Pd is present in square planar coordination with two P and two S atoms (Fig. S1, ESI†). The phosphorous is tetrahedrally coordinated to one S, one P and two Pd atoms while sulphur is tetrahedrally coordinated to one P, two Pd atoms and one lone pair of electrons. The overall structure is reported to be 'layered - type' consisting of pentagons joined to result in puckered two dimensional sheets.[22] Each two adjacent sheets consisting of pentagons are connected through weak P-P bonds. The 'two adjacent sheets' interact with the next 'two adjacent sheets' via weak interactions. Four layers are required to complete one unit cell. The P and S atoms are considered to form polyanions[22] of type $[S\text{-}P\text{-}P\text{-}S]^{4-}$. Recently, Hamidani and Bennecer reported the theoretical calculations of structural, optical and electronic properties of the PdPS.[22] Folmer et.al.[23] reported the photoelectrochemical behavior of PdPS in aqueous medium containing various redox systems and concluded that ferrocyanide / ferricyanide system shows improved performance.

Recent studies reveal that compounds containing sulphur or phosphorous are very active catalysts for HER.[6,8] The present study explores the use of a compound containing both phosphorous and sulphur in the form of a layered semiconducting phospho-chalcogenide. Since the composite of MoS_2 with rGO has been shown to be very active for HER,[16] we have carried out HER studies for bulk PdPS and its composite with rGO.

The as-synthesized PdPS consists of flat-shaped, silvery crystals with sizes ranging from few microns to several microns and the present synthetic protocol yields uniform, pure, single phase material. The formation of single phase crystalline PdPS is confirmed by powder XRD technique that reveals orthorhombic symmetry and the corresponding Rietveld refinement data is shown in figure 1. The highest intense peak at 2θ = 26.67 corresponds to the strong reflection from (400) plane. The calculated lattice parameters (a= 13.3542 Å b= 5.6747 Å c= 5.6939 Å) are similar to the reported [20] values. The crystallite size determined based on the (400) peak, using Scherer equation is

~64 nm. The scanning electron micrograph shown in figure 2a reveals the presence of highly crystalline flaky material with layered structure. The size and shape are found to be polydisperse. The elemental mapping (Fig. S1, ESI†) shows uniform distribution of the three elements and the atomic ratio is found to be ~ 1:1:1 from the EDS analysis. The high-solution TEM image (figure 2b) shows lattice fringes with spacing of 0.336 nm due to the high intense (400) plane of orthorhombic PdPS particles. The selected area electron diffraction pattern (figure 2c) clearly indicates the presence of highly crystalline PdPS. The indexed pattern along [101] zone axis clearly reveals the orthorhombic crystal structure of PdPS.

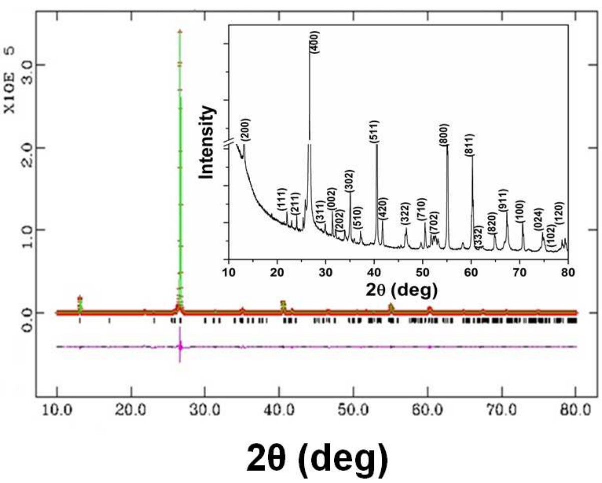

Fig 1. X-ray diffraction pattern of PdPS (green) with Rietveld refined pattern (red). Vertical black lines indicate the Bragg reflections while the intensity difference between the calculated and experimental patterns is shown in pink colour. Inset shows the observed X-ray diffraction pattern for the as-grown crystal with corresponding (hkl) values.

The deconvoluted XPS spectra of PdPS crystal are shown in figure 3. Peaks observed at 335.7 eV and 336.2 eV are due to Pd $3d_{5/2}$ (figure 3a) while the peaks at 340.9 eV and 341.5 eV are due to Pd $3d_{3/2}$ levels. A difference of 5.2 eV due to the spin orbit coupling is clearly observed. Palladium is bonded to P as well as S in addition to weak interactions with other Pd atoms as mentioned earlier. The Pauling electronegativity difference between Pd and P is quite small while the difference between Pd and S is large due to the higher electronegativity value of S than those of P and Pd. This is expected to result in significant changes in the binding energy positions of core level of Pd. The band positions reported for Pd region of palladium sulphide are 336.6 and 341.8 eV.[26] The binding energy values for pure Pd clusters are reported to be around 335.3 eV and 340.0 eV for $3d_{5/2}$ and $3d_{3/2}$ levels.[27] The S 2p (figure 3c) region could be deconvoluted in to two peaks, present at 160.8 eV and 162.1 eV which are due to the S $2p_{3/2}$ and S $2p_{1/2}$ levels respectively. A difference of 1.3 eV is due to the spin orbit coupling. The binding energy value of pure S ($2p_{3/2}$, 164 eV) is expected to decrease when it interacts with Pd as has been reported previously.[26] The P 2p peaks (figure 3b) are observed at 128.6 eV and 129.2 eV. In all three regions, XPS data is quite complex since the bonding is among all the three constituents as mentioned earlier. The composite of PdPS with rGO is characterized by spectroscopic and microscopic techniques. The XRD pattern (Fig. S2, ESI†)

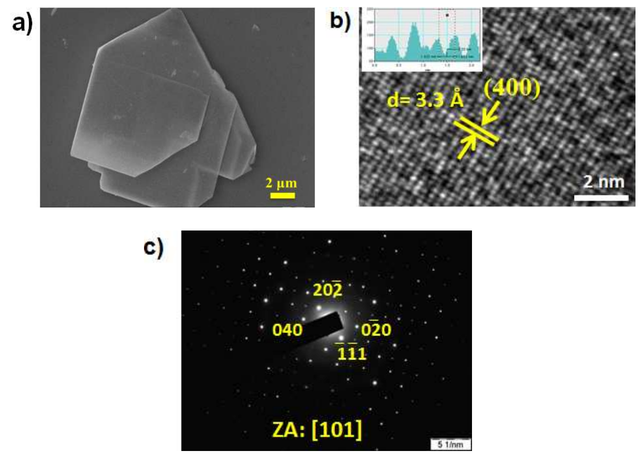

Fig 2. (a) SEM image of PdPS crystal, (b) HRTEM image shows a lattice spacing of 3.3 Å corresponding (400) plane (inset shows the distance) and (c) SAED pattern indexed in [101] zone axis.

shows all the PdPS reflections present in the composite. The microscopy and elemental mapping (Fig. S3 and S4, ESI†) of the rGO-PdPS composite shows PdPS crystals are distributed fairly uniformly over rGO sheets. The XPS data reveal the presence of components of PdPS along with components of rGO (Fig.S5, ESI†). Close examination reveals small shifts in the binding energy values as given in the supporting information (Table S1, ESI†).

Hydrogen evolution activity of PdPS and its composite with rGO have been investigated using a three - electrode set-up. Figure 4a and 4b show the voltammograms where activities for various catalysts are compared. The particle sizes (Fig.S6, ESI†) of MoS_2 and PdPS used in the present studies are very similar, 20 ± 5 µm. It is very clear that bulk PdPS shows higher activity than that of bulk MoS_2 under identical conditions (Figure 4a). The onset potential observed for PdPS is ~ -0.15 V vs RHE which is more positive than the value observed for bulk MoS_2. Few layer MoS_2 (2H polytype) is reported to show an onset of - 200 mV vs. RHE.[28] The electrocatalytic activity is found to be considerably enhanced when PdPS is made in to a composite with rGO. The linear sweep voltammograms observed for bulk PdPS, bulk rGO-PdPS composite and commercial 40 wt% Pt-C catalysts are given in figure 4b. The onset potential for rGO-PdPS is ~ -0.05 V vs RHE while it is ~ 0 V vs RHE in the case of Pt-C.

The HER mechanism is reflected in the Tafel slope involving the following three steps,

1. Volmer: $H^+ + e^- \rightarrow H_{ads}$
2. Heyrovsky: $H_{ads} + H^+ + e^- \rightarrow H_2$
3. Tafel: $H_{ads} + H_{ads} \rightarrow H_2$

wherein Volmer-Heyrovsky mechanism leads to a Tafel slope of ~120 $mVdec^{-1}$, while the slope is expected to be 30 $mVdec^{-1}$ if the mechanism involves Volmer-Tafel steps.[29-31] The Tafel plots obtained in the present studies are shown in figure 4c and it is observed that bulk rGO-PdPS composite shows a slope is 46 $mVdec^{-1}$ while Pt-C shows a Tafel slope at 29 $mVdec^{-1}$ under identical conditions. The exchange current density is determined from Tafel plot to be $1.4x10^{-4} Acm^{-2}$ for the rGO-PdPS. The bulk

PdPS however, shows a Tafel slope of 124 $mVdec^{-1}$ revealing that the mechanism of HER possibly shifts from Volmer-Heyrovsky to Volmer-Tafel when PdPS is made in to a composite with rGO. Various ratios of rGO to PdPS have been tested and it is observed that 50:50 ratio is the optimum value (Fig S7, ESI†). It has been reported that there is an improvement in electrocatalytic activities in batteries, super-capacitors, fuel cells and water electrolyzers when rGO supported catalysts are used.[32] The rGO acts as two-dimensional support matrix for the catalyst and also improves electrical conductivity. The precise mechanism of enhancement with rGO is unclear at present but theoretical studies[33] suggest that strong hybridization between metal d-orbitals and π-orbital of the rGO, extend the density of states of metal d-orbitals. Recently, Ma et al.[34a] reported DFT calculations on graphene – MoS_2 hybrids and concluded that there is a small band gap (2 meV) that is opened up due to the interaction of MoS_2 with graphene. Hydrogen spill over from Pt on to few layer graphene support[34b,c] has recently been reported. The electro-chemical impedance spectroscopic data (Fig. S8, ESI†) shows a charge transfer resistance, R_{CT} of ~300 Ω for rGO-PdPS composite while the value obtained is ~17 KΩ for bulk PdPS.

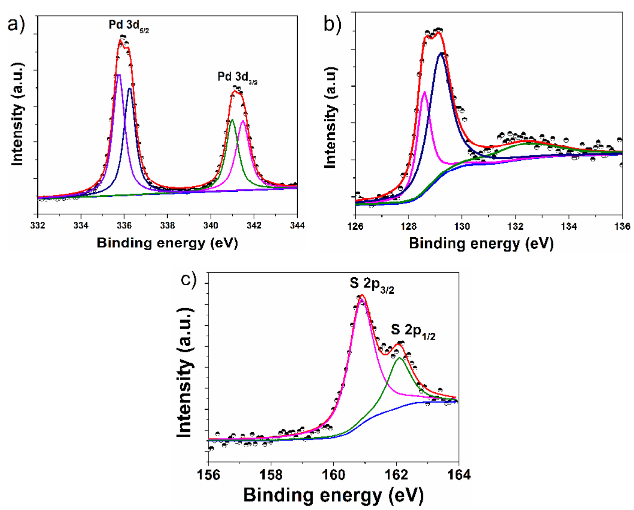

Fig 3. Deconvoluted XPS spectra of (a) Pd-3d, (b) P-2p and (c) S-2p core level regions of bulk PdPS crystal. The experimental data points along with the sum of the spectra are given as well.

The effect of rGO is highly reproducible as in the case of MoS_2-rGO system.[16] Increase in electronic conductivity of the rGO-PdPS as compared to pure PdPS will help in the electron transfer kinetics. The size of PdPS flakes do not change before and after composite formation with rGO. The presence of rGO may help in the adsorption of intermediates (spill over effect) near the catalytic sites thus playing a role in improving the kinetics leading to possible change in mechanism of hydrogen evolution between pure PdPS and rGO-PdPS composite. The changes observed in the binding energy values of the composite lead us to speculate that there is an interaction between rGO and P / S of PdPS thus affecting the HER activity. This aspect needs further investigation to understand the rGO / catalyst interface.

Stability of the electrocatalyst is an issue when gas evolution occurs on the electrode surface. It has been pointed out that Ni-Mo nanopowder which is one of the best HER catalysts reported so far, degrades during continuous operation.[35] The rGO-PdPS catalyst is cycled between +0.25 V and -0.45 V (vs RHE) at a scan rate of 100 mVs^{-1} for a large number of cycles. The stability of the catalyst is shown in figure 4d where the voltammograms almost overlay with each other in the 1st and 1000th cycles. The XRD patterns of the electrode material examined before and after 1000 cycles (Fig. S9, ESI†) reveals no structural change during operation. The morphology and

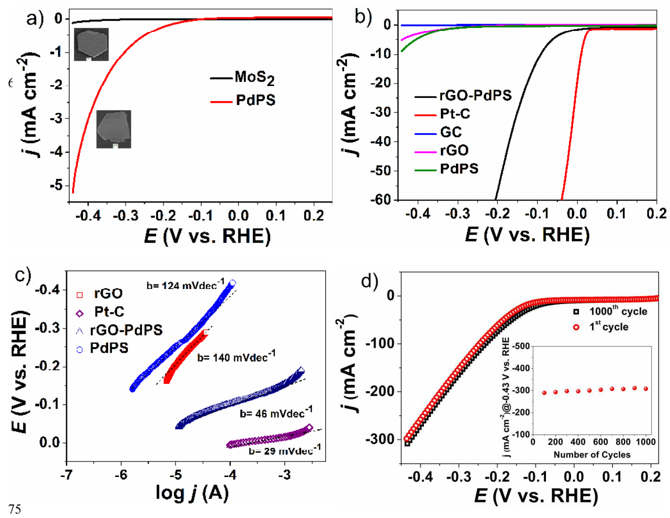

Fig 4. a) Linear sweep voltammograms of bulk MoS_2 and bulk PdPS in 0.5 M H_2SO_4 solution. Insets show the sizes of the flakes used are very similar. (b) Linear sweep voltammograms of rGO, bulk PdPS, rGO-PdPS composite and 40 wt% Pt-C in 0.5 M H_2SO_4 solution (pH 0.8); Scan rate used is 1 mVs^{-1} and the catalyst loading is 2.5 $mgcm^{-2}$ except in the case of Pt-C (0.285 $mgcm^{-2}$). Please note that the scale on the y-axis are different in figures a and b. (c) Tafel plots for PdPS, rGO, rGO-PdPS and 40 wt% Pt-C in 0.5 M H_2SO_4. (d) Linear sweep voltammograms of rGO-PdPS composite on GC electrode before and after 1000 cycles, at 100 mVs^{-1} scan rate. Stability of rGO-PdPS catalyst at overpotential of -0.43 V is shown as currents observed as a function of no. of cycles.

atomic ratio of the constituents of the catalyst are retained as well (Fig. S10, ESI†), implying excellent stability of the rGO-PdPS composite in the acidic medium during HER. The amount of hydrogen gas evolved is quantified with respect to the faradaic efficiency using a H-shaped electrochemical cell where the working and counter electrodes are separated. The quantity of hydrogen gas evolved is measured with time and as shown in the supporting information (Fig. S11, ESI†), the amount of hydrogen evolved is close to that of the theoretical value based on the charge passed.

The overpotential required for the rGO-PdPS catalyst to achieve 10 $mAcm^{-2}$ cathodic current density is ~ 90 mV vs. RHE, relative to the geometric area of the electrode. This value is small as compared to other non - Pt based HER electro-catalysts in aqueous acidic medium. The comparison with the literature data is difficult since the mass loadings are not the same. The bulk Mo_2C and Mo_2C nanoparticles on CNTs,[9] MoB,[10] nanosized MoS_2 on rGO,[16] unsupported Ni-Mo-N nanosheets,[36] Ni-Mo nanopowder[35] and NiP_2 nanoparticles.[8] exhibit over-potentials in the range of 140- 240 mV to produce 10 – 20 $mAcm^{-2}$ cathodic current densities (Table S2, ESI†). The number of catalytically active sites and turn over frequency (TOF) have been determined based on a reported procedure.[37] The TOF obtained is 0.3 s^{-1} for rGO-PdPS at $\eta = 0.1$ V versus RHE. The value of TOF reported for NiP_2 at 0.015 s^{-1} at $\eta = 0.1$ V vs. RHE[8] while for MoS_2 / CNT hybrid, the TOF value reported is 0.06 s^{-1} at $\eta = 0.0$ V.[37]

In summary, the present studies reveal that PdPS acts as a good catalyst for HER and the efficiency is enhanced by the presence of rGO. The participation of S edges is well understood[15] based on MoS_2 systems. It has been indicated in the case of Pd-P alloys[38] that P possibly plays a role in hydrogen adsorption. The bulk PdPS being active for HER for large number of cycles also reveals that intercalation of hydrogen proposed in the case of bulk MoS_2 does not occur in the case of PdPS. In addition, preliminary studies indicate that the characteristics for under potential deposition of hydrogen are different on PdPS and bulk Pd and this is being investigated. Use of few layer PdPS may improve the HER activity further and is currently studied.

Notes and references

Department of Inorganic and Physical Chemistry, Indian Institute of Science, Bangalor-560012e, India. Fax: +91-80-2360-0085; Tel: +91-80 2293 3315; E-mail: sampath@ipc.iisc.ernet.in

† Electronic Supplementary Information (ESI) available: Detailed experimental procedures and techniques, additional characterization data and tabular form of comparative studies with other catalysts are included in the supporting information. See DOI: 10.1039/b000000x/

1 N. S. Lewis, D. G. Nocera, *Pro. Natl. Acad. Sci. U.S.A,* 2006, **103**, 15729.

2 M. G. Walter, E. L. Warren, J. R. McKone, S. W. Boettcher, Q. Mi, E. A. Santori, N. S. Lewis, *Chem. Rev.,* 2010, **110**, 6446.

3 M. M. Jaksic, *Int. J. Hydrogen Energy,* 2001, **26**, 559.

4 J. K. Nørskov, T. Bligaard, A. Logadottir, J. R. Kitchin, J. G. Chen, S. Pandelov, U. Stimming, *J. Electrochem. Soc.,* 2005, **152**, J23.

5 D. Kong, J. J. Cha, H. Wang, H. R. Lee, Y. Cui, *Energy Environ. Sci.,* 2013, **6**, 3553.

6 a) D. Merki, X. Hu, *Energy Environ. Sci.,* 2011, **4**, 3878; b) Z. Wu, B. Fang, A. Bonakdarpour, A. Sun, D. P. Wilkinson, D. Wang *Appl. Catal. B: Environmental,* 2012, **125**, 59.

7 a) D. Kong, H. Wang, J. J. Cha, M. Pasta, K. J. Koski, J. Yao and,Y. Cui, *Nano Lett*., 2013, **13**, 1341; b) H. Wang, D. Kong, P. Johanes, J. J. Cha, G. Zheng, K. Yan, N. Liu and Y. Cui, *Nano Lett.,* 2013, **13**, 3426.

8 a) E. J. Popczun, J. R. McKone, C. G. Read, A. J. Biacchi, A. M. Wiltrout, N. S. Lewis, R. E. Schaak, *J. Am. Chem. Soc.,* 2013, **135**, 9267; b) I.Paseka, *Electrochim. Acta*, 1995, **40**, 1633

9 W. F. Chen, C. H. Wang, K. Sasaki, N. Marinkovic, W. Xu, J. T. Muckerman, Y. Zhu, R. R. Adzic, *Energy Environ. Sci.,* 2013, **6**, 943.

10 H. Vrubel, X. Hu, *Angew.Chem.,* 2012, **124**, 12875.

11 J. Greeley, J. K. Nørskov, L. A. Kibler, A. M. El-Aziz, D. M. Kolb, *ChemPhysChem,* 2006, **7**, 1032.

12 a) W. Jaegermann, H. Tributsch, *Prog. Surf. Sci.* **1988**, *29*, 1-167; b) L. B. Albertini, A. C. D. Angelo, E. R. Gonzalez, *J Appl. Electrochem.,* 1992, **22**, 888.

13 a) B. Hinnemann, P. G. Moses, J. Bonde, K. P. Jørgensen, J. H. Nielsen, S. Horch, I. Chorkendorff, J. K. Nørskov, *J. Am. Chem. Soc*., 2005, **127**, 5308; b) D. Y. Chung, S.-K. Park, Y.-H. Chung, S.-H. Yu, D.-H. Lim, N. Jung, H. C. Ham, H.-Y. Park, Y. Piao, S. J. Yoo, Y.-E. Sung *Nanoscale,* 2014, DOI: 10.1039/C3NR05228A

14 T. F. Jaramillo, K. P. Jørgensen, J. Bonde, J. H. Nielsen, S. Horch, I. Chorkendorff, *Science,* 2007, **317**, 100.

15 W.-F. Chen, S. Iyer, S. Iyer, K. Sasaki, C.-H. Wang, Y. Zhu, J. T. Muckerman, E. Fujita, *Energy Environ. Sci*., 2013, **6**, 1818.

16 a) Y. Li, H. Wang, L. Xie, Y. Liang, G. Hong, H. Dai, *J. Am. Chem. Soc.,* 2011, **133**, 7296; b) L. Liao , J. Zhu , X. Bian , L. Zhu , M. D. Scanlon , H. H. Girault , B.Liu, *Adv. Funct. Mater*. 2013, **23**, 5326.

17 I. A.Pasti, N. M. Gavrilov, S. V. Mentus, *Adv. Phys. Chem.,* 2011, **2011**, 8.

18 M. Johansson, E. Skúlason, G. Nielsen, S. Murphy, R. M. Nielsen, I. Chorkendorff, *Surf. Sci.,* 2010, **604**, 718.

19 F. Al-Odail, A. Anastasopoulos, B. Hayden, *Top Catal,* 2011, **54**, 77.

20 T. A. Bither, P. C. Donohue, H. S. Young, *J. Solid State Chem.,* 1971, **3**, 300.

21 a) W. Jeitschko, *Acta Crystallogr., Sect. B,* 1974, **30**, 2565; (b) A. J. Foecker, W. Jeitschko, *J. Solid State Chem*., 2001, **162**, 69; (c) J. K. Burdett, B. A. Coddens, *Inorg. Chem.,* 1988, **27**, 418

22 A. Hamidani, B. Bennecer, *Comput. Mater. Sci.,* 2010, **48**, 115.

23 J. C. W. Folmer, J. A. Turner, B. A. Parkinson, *J. Solid State Chem.,* 1987, **68**, 28.

24 P. Ramesh, S. Bhagyalakshmi, S. Sampath, *J. Colloid Interface Sci.,* 2004, **274**, 95.

25 M.-R. Gao, Z.-Y. Lin, T.-T. Zhuang, J. Jiang, Y.-F. Xu, Y.-R. Zheng, S.-H. Yu, *J. Mat. Chem.,* 2012, **22**, 13662.

26 R. Bhatt, S. Bhattacharya, R. Basu, A. Singh, U. Deshpande, C. Surger, S. Basu, D. K. Aswal, S. K. Gupta, *Thin Solid Films,* 2013, **539**, 41.

27 NIST x-ray photoelectron spectroscopic data, NIST, USA, Web page: http://srdata.nist.gov/xps/.

28 a) M. A. Lukowski, A. S. Daniel, F. Meng, A. Forticaux, L. Li, S. Jin, *J. Am. Chem. Soc.,* 2013, **135**, 10274; b) J.Xie, J. Zhang, S.Li, F. Grote, X.. Zhang, H.Zhang, R. Wang, Y. Lei, B. Pan,Y. Xie, *J. Am. Chem. Soc*. 2013, **135**, 17881; c) J.Xie , H. Zhang , S. Li , R. Wang , X.Sun , M. Zhou , J.Zhou ,X. W.Lou , Y.Xie, *Adv. Mater*. 2013, **25**, 5807.

29 N. Pentland, J. O. M. Bockris, E. Sheldon, *J. Electrochem. Soc.,* 1957, **104**, 182.

30 W. Sheng, H. A. Gasteiger, Y. Shao-Horn, *J. Electrochem. Soc*., 2010, **157**, B1529.

31 B. E. Conway, B. V. Tilak, *Electrochim. Acta,* 2002, **47**, 3571.

32 Y. Liang, Y. Li, H. Wang, H. Dai *J. Am. Chem. Soc*., 2013, **135**, 2013.

33 a) C. Gong, G. Lee, B. Shan, E. M. Vogel, R. M. Wallace, K. Cho, *J. Appl. Phys.,* 2010, **108**,123711.

34 a) Y. Ma, Y. Dai, M. Guo, C. Niu, B. Huang, *Nanoscale,* 2011, **3**, 3883; b) S.Mukherjee, B.Ramalingam, S . Gangopadhyay, *J. Mater. Chem A*., 2014**,** DOI: 10.1039/b000000x c) G. M. Psofogiannakis, G.E. Froudakis, *Chem.Commun.,* 2011, **47**, 793334.

35 J. R. McKone, B. F. Sadtler, C. A. Werlang, N. S. Lewis, H. B. Gray, *ACS Catl.,* 2012, **3**, 166.

36 W.F. Chen, K. Sasaki, C. Ma, A. I. Frenkel, N. Marinkovic, J. T. Muckerman, Y. Zhu, R. R. Adzic, *Angew. Chem. Int. Ed.,* 2012, **51**, 6131.

37 Y. Yan, X. Ge, Z. Liu, J-Y.Wang, J.M. Lee, X. Wang, *Nanoscale* 2013, **5**. 7768.

38 E. Robertisa, A. M. Fundo, A.J. Motheo, L. M. Abrantes, *J. Braz. Chem. Soc.,* 2005, **16**, 103.

Table of content entry

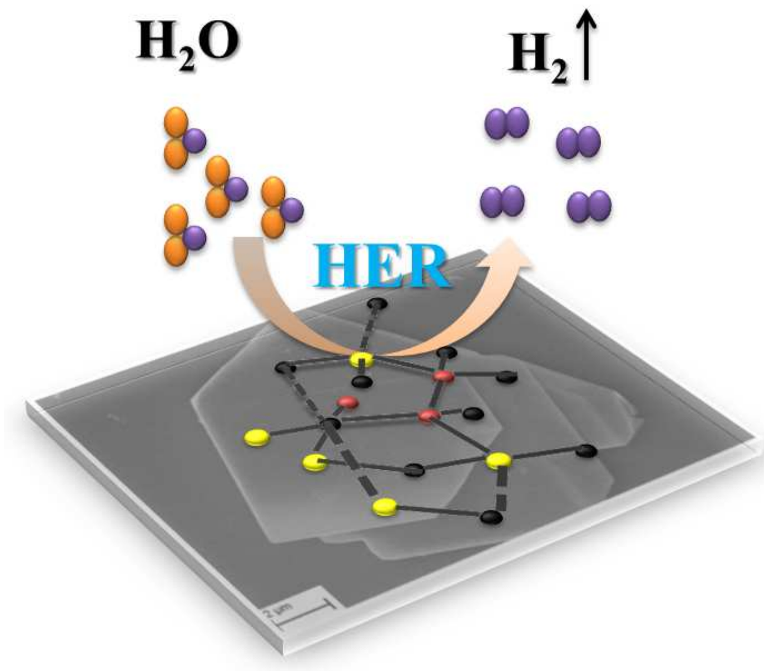

PdPS - rGO composite is an excellent catalyst for HER